Available online at www.sciencedirect.com
ScienceDirect
Science of the Total Environment 370 (2006) 168–181
Science of the Total Environment
An International Journal for Scientific Research into the Environment and its Relationship with Humankind
www.elsevier.com/locate/scitotenv

Mapping of spatial multi-scale sources of arsenic variation in groundwater on ChiaNan floodplain of Taiwan

Yun-Bin Lin [a], Yu-Pin Lin [b,*], Chen-Wuing Liu [c], Yih-Chi Tan [d]

[a] *Department of Recreation and Health-Care Management, ChiaNan University of Pharmacy and Science, Rende Shiang, Tainan County 71710, Taiwan, ROC*
[b] *Department of Bioenvironmental Systems Engineering, National Taiwan University, 1 Sec. 4 Roosevelt Road, Taipei 10673, Taiwan, ROC*
[c] *Department of Bioenvironmental Systems Engineering, National Taiwan University, Taipei 10673, Taiwan, ROC*
[d] *Department of Bioenvironmental Systems Engineering, and Hydrotech Research Institute, National Taiwan University, Taipei 10673, Taiwan, ROC*

Received 1 December 2005; received in revised form 23 June 2006; accepted 2 July 2006
Available online 9 August 2006

Abstract

This study applied multivariate factorial kriging to derive the characteristics of the spatial variations of groundwater arsenic distributions at different scales on the ChiaNan floodplain, Taiwan. Seven variables (dissolved oxygen, oxidation-reduction potential, alkalinity, sulfate, iron cations, manganese cations and total organic carbon) and Arsenic were adopted to analyze the mechanisms of arsenic enrichments in groundwater. The hydrogeological environment had spatial and quantitative influences on arsenic enrichments at different scales. The regional scale was set to 32 km referring to the extension distance of flow paths to reflect the effects of flushing in the aquifer, while the local scale was set to 16 km referring to the farthest distance of seawater intrusion to determine the influence of seawater intrusion. The results of factorial kriging suggested that arsenic releases resulted partially from pyrite oxidation during the flushing at the regional scale and partially due to the siderite dissolution at the local scale. Overall, the alkalinity dominated arsenic distribution in groundwater at both the regional and local scales. The multivariate factorial kriging results also demonstrated that seawater intrusion slightly affected the increase of arsenic in groundwater, accounting for only 17.3% of total variation. However, the interaction of seawater intrusion and arsenic distribution in space indicated that seawater intrusion restrained the distribution of arsenic from the areas where seawater was located. High dissolved oxygen was found at where over-pumping induced drawdown cones occurred and also limited the spatial variation of arsenic. Our findings indicate that multivariate factorial kriging can be a useful mapping tool to improve understanding of the mechanism of arsenic release in groundwater at different scales. And the results conducted from the application of multivariate factorial kriging in southwestern Taiwan reveal the important influences of the hydrogeological processes, either artificial or natural, on the arsenic variations in groundwater.

Keywords: Multivariate factorial kriging; Spatial sources of arsenic variation; Arsenic contamination of groundwater; Flushing; Seawater intrusion

1. Introduction

Black foot disease was generally found on the ChiaNan floodplain during the early 1960s. This disease

* Corresponding author. Tel.: +886 2 2368 6980; fax: +886 2 2368 6980.
E-mail address: yplin@ntu.edu.tw (Y.-P. Lin).

0048-9697/$ - see front matter © 2006 Elsevier B.V. All rights reserved.
doi:10.1016/j.scitotenv.2006.07.002

was found to be strongly correlated with the direct ingestion of high arsenic (As) groundwater from deep wells mostly screened 100–280 m below ground. Large amounts of data whose subjects were assigned exposures according to exposure categories instead of having individual measurements of As exposures was collected in southwestern Taiwan and the data was generally recognized as the ecological data (Tseng et al., 1968; Chen et al., 1994; Guo and Valberg, 1997). The statistical analysis of ecological data initiated the quantitative risk assessment of cancer mortality of skin cancer and some internal cancers, including lung, bladder and liver due to chronic ingestion of As in groundwater. The assessment was adopted to define the maximum contaminant level of drinking water (National Research Council 1999, 2001). The World Health Organization (World Health Organization, 1993) and the U.S. EPA (National Research Council, 2001) reduced As standards for drinking water from 50 to 10 ppb after consulting studies regarding the carcinogenicity of As in drinking water conducted in southwestern Taiwan.

At present, the groundwater is not the primary sources for direct ingestion or domestic use in Taiwan. However, the study concerning the statistical correlations between high As and seawater samples in littoral zones in Taiwan which was done by Liu et al. (2003) via conventional factor analysis motivates further investigation of spatial correlations between distributions of As and seawater intrusion via geostatistics. Aquaculture is the primary agricultural sector in the littoral zones in southwestern Taiwan, including the ChiaNan floodplain. Groundwater provides a stable and low priced source of water. Large quantities of groundwater have been extracted from the aquifer to meet fishpond needs. The serious seawater intrusion problem was induced by these extractions. The seawater intrusion seemed to restrain the distribution of As from the areas where seawater was located. Pumping from high As area raises a serious issue of edible safety of aquaculture products in the littoral zones of southwestern Taiwan.

The variation of As in groundwater is complex, Smedley and Kinniburgh (2002) established the classification table which lists the risk factors being tested with the highest priority in various hydrogeological environments. The variations of As in groundwater are related to past and present hydrogeological conditions, which may include the flushing process in aquifers, and seawater intrusion induced by over pumping. These artificial or natural hydrogeological processes perform at different scales. Hossain and Sivakumar (2006) used the chaotic analysis to determine the dimensions of the spatial variability of As in groundwater. The value of dimensions represents the number of variables needed in modeling the spatial variability of As in groundwater and was found to be highly correlated with the sampling interval. The analytical results indicated that different mechanisms involve in at different scales. The assessment of the oncoming risk of cancer incidence due to As exposures relies on the understanding of the release mechanism at different scales which generates the fluctuations of As concentrations over time in groundwater. Mapping of multivariate spatial variation of groundwater quality can effectively improve our understanding of the As release mechanism at different scales and clarify the spatial relationships between the disease and groundwater As in Taiwan. Moreover, the results of multivariate spatial analysis can also be applied to support the management of water containment and ensure the edible safety of aquaculture products in the littoral zone of southwestern Taiwan.

Geostatistical methods, such as kriging, provide a linear un-biased estimate at the unsampled grid nodes. The estimates are weighted sums of the adjacent sampled variables. The weights are determined by the spatial structures of experimental variograms and are selected by minimizing the estimation variance (Cressie, 1990; Wackernagel, 1995). Spatial structures of experimental variograms are modeled using the linear combination of various allowable basic models with different ranges. The modeling procedure is also termed 'regionalization' in the univariate case and 'co-regionalization' in the multivariate case. Moreover, the modeled matrix of the experimental variograms should be positive semi-definite in the multivariate case (Goovaerts et al., 1993; Goovaerts, 1997). Goulard and Voltz (1992) proposed the linear model of coregionalization (LMC) to minimize the weighted sum of the squared differences between the experimental variogram and the variogram model, and to maintain the positive semi-definition of the modeled matrix. The LMC resulting matrices at different scales or ranges were then applied to principal component analysis (PCA) to examine the relationships between variables at each scale. Finally, the spatial variations of the principal components at different scales, regionalized factors, are mapped by factorial kriging. The dominant causation generating the relationships between variables is then deduced from the PCA results and maps of regionalized factors. Therefore, the spatial variations of multivariables associated with various processes at different scales can be distinguished via Multivariate factorial kriging (MFK) which is a multivariate geostatistical method for dealing with multivariate problems with

various scales and comprises three steps: LMC, PCA and mapping (Castrignanò et al., 2000).

Recently, MFK has been widely used in many fields, including seismology (Lin et al., 2004), geochemistry (Smedley and Kinniburgh, 2002; Bourennane et al., 2003; Reis et al., 2003), remote sensing (Van Meirvenne and Goovaerts, 2002; Goovaerts et al., 2005b), and contamination assessment (Lin, 2002; Goovaerts et al., 2005a). In previous notable studies on As, Gaus et al. (2003) and Reis et al. (2005) used disjunctive kriging and indicator kriging, respectively, to estimate As concentrations in groundwater and map the exceeding probability of the national safety standards for As in drinking water. Yu et al. (2003) reported that much of the large scale variation of As in groundwater over the entire Bangladesh is explained by differences in geology and geomorphology, while small scale variation results primarily from well depth. The As affected aquifers in Bangladesh are reductive with clayey deposits, young (of Holocene age) and shallow (100–150 m below the ground) while the ones in southwestern Taiwan are also reductive with clayey deposits but elder (of Pleistocene age) and deeper (100–280 m below the ground). The similar environment implies the possible scale influences of hydrogeology on the As enrichment in southwestern Taiwan. Goovaerts et al. (2005a) applied MFK to filter out large scale variability in As concentrations, and found that the variations are correlated with types of unconsolidated deposits. These studies indicated that multivariate factorial kriging, which could efficiently extract the spatial variations of variables with different scales and construct the spatial correlations between variables, was suitable for analyzing the mechanism of As release in groundwater at different scales.

The variation of As in groundwater may be accumulatively affected by hydrogeological processes or chemical reactions at different scales. Since only the outcomes of As variations can be observed in the field, it is essential to decompose the lumped variations of individual observations into componential variations at different scales to clarify the causation of variations at different scales. This study used MFK to analyze and map the spatial relationships between seven variables of groundwater quality and As on the ChiaNan floodplain. The possible interactions between hydrogeological factors which induced the spatial variations of As distribution at different scales were evaluated by principal component analysis. The additional hydrogeological surveys were also proposed to justify the mapping results of regionalized factors. The mapping results were also used to discuss the influence of seawater intrusion on spatial characteristics of distributions of As variations. The MFK results reveals the whole pictures of key factors which dominate the As variations in groundwater, from a geostatistical perspective, and provides the possible inferences for further deterministic geochemistry approval.

2. Materials and methods

2.1. Materials

The ChiaNan floodplain, shown in Fig. 1, is the study area used to assess the multi-scale anomalies of spatial variation of the As distributions in groundwater. The ChiaNan floodplain is located in southwestern Taiwan and covers around 2400 km^2. The plain extends 40 km from east to west and 60 km from north to south. The upstream of the rivers serving the floodplain flow through Miocene to Pleistocene rocks with a fine texture. Since 1992, the Water Resources Agency established a Groundwater Monitoring Network System (GMNS) for monitoring groundwater quality and quantity and land subsidence in Taiwan (Hsu, 1998). The network on the ChiaNan floodplain includes 40 evenly distributed hydrogeological stations, comprising 108 monitoring wells with various depths ranging from 4 to 289 m. Groundwater quality samples were collected from 33 stations (Fig. 1) including 100 wells in the study area (Taiwan Sugar Corporation, 2001).

The hydrogeological profiles display no clear layer structure, as illustrated in Fig. 2(a). However, the hydrogeological environment is still roughly divided into five aquifers, based on characteristics of geological age, with 0–60 m below ground assigned to Aquifer 1, 60–140 m below ground assigned to Aquifer 2, 140–200 m below ground assigned to Aquifer 3, 200–250 m below ground assigned to Aquifer 4 and 250–300 m below ground assigned to Aquifer 5, from top to bottom. Sediments in Aquifers 2 to 5 are formed by Miocene to Pleistocene sands and silt mixed with marine mud, while Aquifer 1 was formed by the Holocene deposits. Accordingly the deposits dated 10 thousand years ago (ka) is adopted as the interface between Aquifers 1 and 2. The lowest mean sea level at the last glacial epoch (20 ka) is adopted as the interface between Aquifers 2 and 3. Therefore the aquifers below Aquifer 2 had previously experienced a much greater hydraulic gradient than they presently faced. The higher hydraulic gradient can cause extensive aquifer flushing. Because groundwater in Aquifers 3 to 5 is fresh water owing to the flushing, water was mostly extracted from Aquifer 3 for aquaculture use in the littoral zones (Liu, 1999).

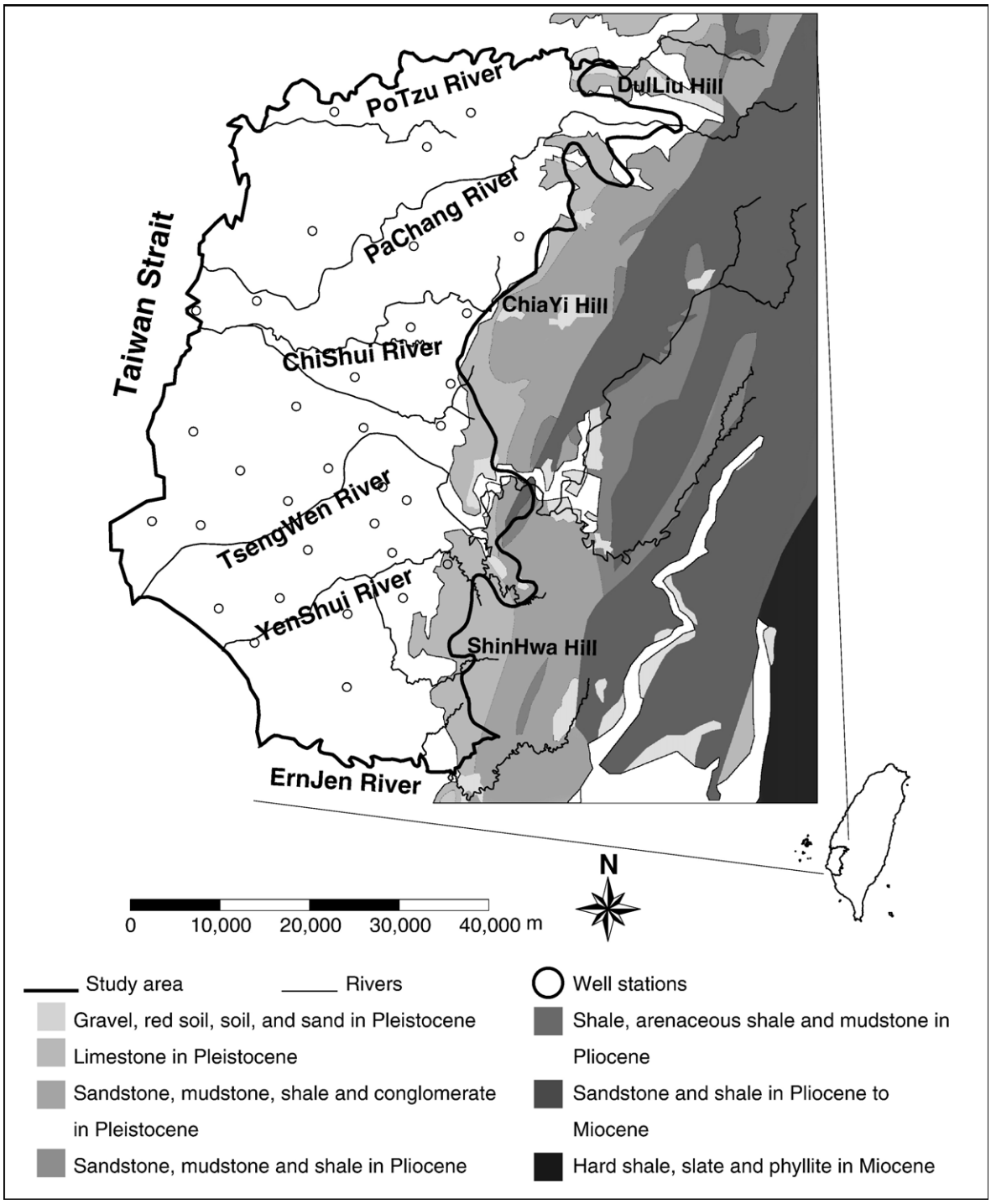

Fig. 1. Geography and geology of the ChiaNan floodplain and well stations of GMNS.

Groundwater quality samples obtained from 22 wells screened in Aquifer 3 (Fig. 2(b)) were used to assess the influence of flushing and seawater intrusion on the spatial distribution of As. That no artificial tritium (^3H) can be found in Aquifer 3 indicates no anthropogenic sources of As in the aquifer (Liu, 1999). Eight variables including Dissolved Oxygen (DO), Oxidation Reduction Potential (ORP), Alkalinity (Alk), sulfate (SO_4^{2-}),

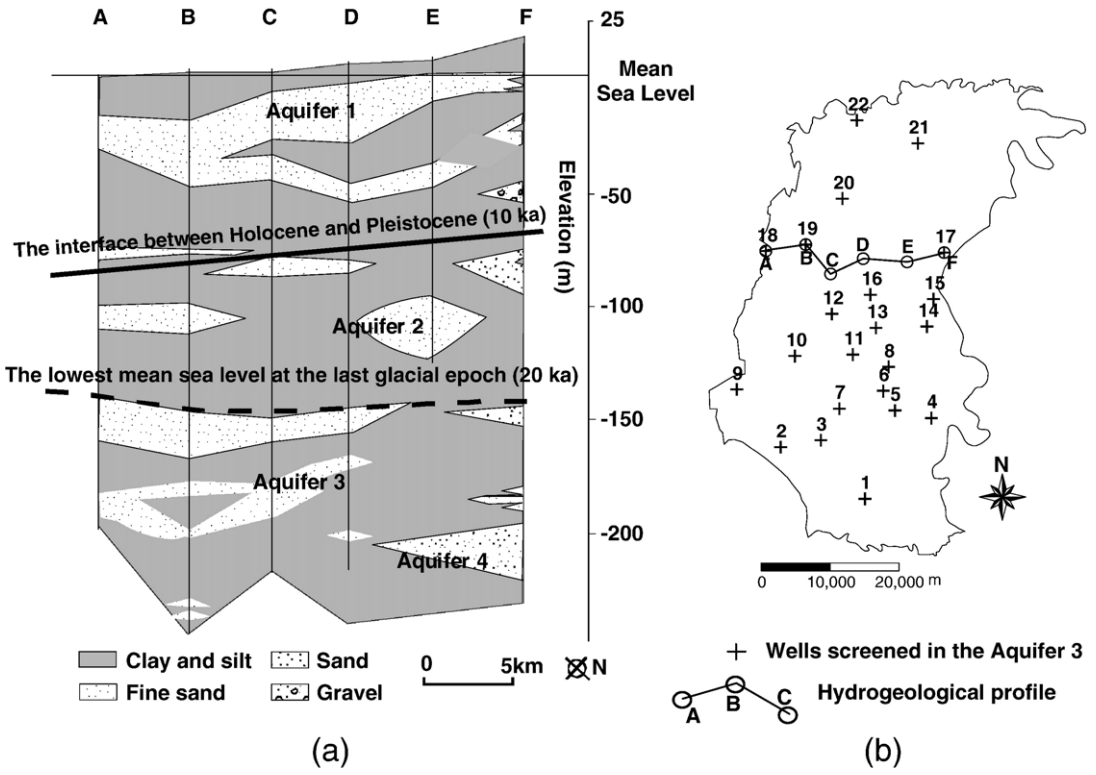

Fig. 2. (a) The hydrogeological profile of the ChiaNan floodplain and (b) wells screened in Aquifer 3.

iron cations (Fe), manganese cations (Mn), total organic carbon (TOC) and As were chosen referring to the classification table (Smedley and Kinniburgh, 2002) which lists the risk factors being tested with the highest priority in the reduced environment of the aquifer with low flushing rate. Table 1 lists the analytical methods, detection limits, raw data from the 22 well samples, and descriptive statistics of all variables. Most variables are analyzed in the laboratory, except for DO and ORP. Two distinct histogram types exist. Histograms of SO_4^{2-}, Fe, Mn and TOC exhibit large positive skewness and kurtosis. Moreover, the histogram of SO_4^{2-} has the largest positive skewness and kurtosis. The histograms of DO and ORP closely approach the normal distribution. The shape of the As histogram lies between these two types. All variables are initially normalized with zero mean and unit variance to prevent estimation bias. Table 2 lists the correlation matrix of eight variables.

2.2. Methods

2.2.1. Variography

The scales must be chosen in advance for modeling the experimental variograms and determining the regionalized factors. The physical meanings of setting scales result from knowledge of natural processes at different scales (Goovaerts, 1997). In the first step of variography, data were initially decomposed horizontally into the local scale and the regional scale. The variations of As within the longest extension in the east–west direction were adopted to explore the influence of flushing on As distribution in groundwater. The longest west–east extension of the study area was around 40 km, and the regional scale was set to 80% of the extension, 32 km. Moreover, the variations at the local scale were hypothesized to be influenced by seawater intrusion. Piper plot was used to locate seawater intrusion. Fig. 3(a) shows the Piper plot (Appelo and Postma, 1994) of the 22 well samples in Aquifer 3. Eight well samples (#10, #9, #12, #11, #3, #16, #7 and #1, from closest to farthest) are highly correlated with seawater in quadrant III. The directions of seawater intrusion are also labeled in Fig. 3(b). Another 12 well samples (#2, #4, #5, #6, #8, #13, #14, #15, #17, #18, #21 and #22) are $NaHCO_3$ type water, presenting salt water being flushed by fresh water, as labeled in quadrant II. And the #19 and #20 well samples represent the mixed type of $NaHCO_3$ type water and seawater. The local scale was set to 16 km, being 80% of the

Table 1
Analytical methods, detection limits, raw data, and descriptive statistics of all variables

Variables	As	DO	ORP	Alk	SO_4^{2-}	Fe	Mn	TOC
Dimensions	mg/l	mg/l	mV(at 25 °C)	mg/l	mg/l	mg/l	mg/l	mg/l
Analytical methods	NIEA[b] W310.50 A	APHA[c] (20th) 4500 OG	APHA(20th) 2580 B	APHA(19th) 2320 B	NIEA W430.50 A	TDS < 1000 mg/l NIEA W 306.50 A TDS > 1000 mg/l NIEA W309.20 A	TDS < 1000 mg/l NIEA W 306.50 A TDS > 1000 mg/l NIEA W309.20 A	NIEA W530.50 C
Detection limits	0.011	0.00–19.99	± 1999 mV	15	1.01	0.057	0.04	0.2
Measured place	Lab. anal.	In situ	In situ	Lab. anal.	Lab. anal.	Lab. anal.	Lab. anal.	Lab. anal.
Well number	Raw data							
1	0.16	0.08	−230	335	6.9	0.09	0.09	1.39
2	1.12	0.17	−240	715	122.0	25.03	0.63	10.28
3	0.62	0.06	−358	670	685.0	0.08	0.20	6.20
4	0.02	0.18	−142	305	11.6	0.38	0.13	0.90
5	0.02	0.17	−54	415	11.1	0.91	0.18	1.30
6	0.37	–[d]	–[d]	515	1.03	3.24	0.04	3.44
7	1.20	0.11	−234	660	23.3	2.35	0.09	9.56
8	0.02	0.38	−197	370	2.5	0.20	0.11	1.31
9	1.14	0.14	−404	1175	1048.0	62.93	0.51	24.08
10	0.14	0.19	−282	440	32.5	78.96	0.13	10.95
11	0.44	0.40	−198	400	2.9	9.51	0.20	6.26
12	0.92	0.33	−260	400	13.9	1.40	0.03	8.70
13	0.03	0.29	−181	370	2.7	0.16	0.20	1.43
14	0.04	0.24	−133	475	23.0	0.13	0.12	1.55
15	0.07	0.28	−219	420	5.8	0.61	0.09	1.23
16	0.28	0.33	−197	710	6.4	2.09	0.11	13.51
17	0.23	0.25	−203	390	3.8	0.78	0.68	1.64
18	0.55	0.18	−294	835	14.9	1.37	0.03	9.41
19	0.37	0.24	−254	645	24.2	2.22	0.09	5.01
20	0.13	0.28	−188	450	27.4	0.15	0.04	5.95
21	0.12	–[d]	–[d]	400	35.8	2.28	0.21	1.06
22	0.70	–[d]	–[d]	565	4.3	0.97	0.19	1.47
Descriptive statistics								
Sample numbers	22	19	19	22	22	22	22	22
Mean	0.395	0.226	−224.6	530.0	95.87	8.902	0.186	5.756
Median	0.255	0.240	−219.0	445.0	12.75	1.170	0.124	4.225
Standard deviation	0.395	0.097	78.5	204.7	256.89	20.937	0.183	5.702
Skewness[a]	0.976	0.078	−0.287	1.678	3.264	2.835	1.922	1.722
Kurtosis[a]	−0.301	−0.701	1.256	3.446	10.252	7.325	2.925	3.830
Maximum	1.20	0.40	−54	1175	1048	78.96	0.68	24.08
Minimum	0.02	0.06	−404	305	1.03	0.08	0.03	0.90
25th percentile	0.083	0.170	−257.0	400.0	4.66	0.245	0.087	1.400
75th percentile	0.603	0.285	−192.5	656.3	26.60	2.333	0.201	9.233

[a] Zero for the normal distribution.
[b] NIEA: National Institute of Environmental Analysis, Environmental Analysis Laboratory, Environmental Protection Administration, Taiwan.
[c] APHA: American Public Health Association, American Water Works Association and Water Pollution Control Federation, U.S.A.
[d] '–' represents no in-situ test.

farthest intrusion distance, 20 km. The software VARIOWIN (Pannatier, 1996) was then used to model the experimental variograms.

2.2.2. Multivariate factorial kriging

The direct and the cross experimental variograms of n variables, $\mathbf{\Gamma}(h)=[\gamma_{ij}(h)]$, can be modeled with a

Table 2
Correlations matrix

	As	DO	ORP	Alk	SO_4^{2-}	Fe	Mn	TOC
As	1	−0.322	−0.624	0.685	0.472	0.268	0.324	0.665
DO		1	0.343	−0.354	−0.444	−0.205	−0.159	−0.171
ORP			1	−0.686	−0.718	−0.502	−0.192	−0.694
Alk				1	0.711	0.414	0.292	0.831
SO_4^{2-}					1	0.471	0.394	0.649
Fe			Symmetry			1	0.320	0.669
Mn							1	0.254
TOC								1

linear combination of various basic allowable models at various scales of l, given by $g^l(h)$, where $\mathbf{\Gamma}(h)$ has dimensions of $n \times n$. The co-regionalization method is expressed as

$$\boldsymbol{\Gamma}(h) = [\gamma_{ij}(h)] = \sum_l \mathbf{B}^l g^l(h),$$

where $\mathbf{B}^l$ must be a positive semi-definite matrix for each scale l and each has dimensions of $n \times n$. Goulard (1989) proposed the minimization of the squared difference between the experimental and modeled values in variograms to determine the positive semi-definite co-regionalization matrix. Goulard and Voltz (1992) later suggested that the weighted sum of squares (WSS) is optimal in fitting. However, WSS may yield a deviation between the direct experimental variograms and variogram models, so the result of modeling should be visually checked (Goovaerts, 1997).

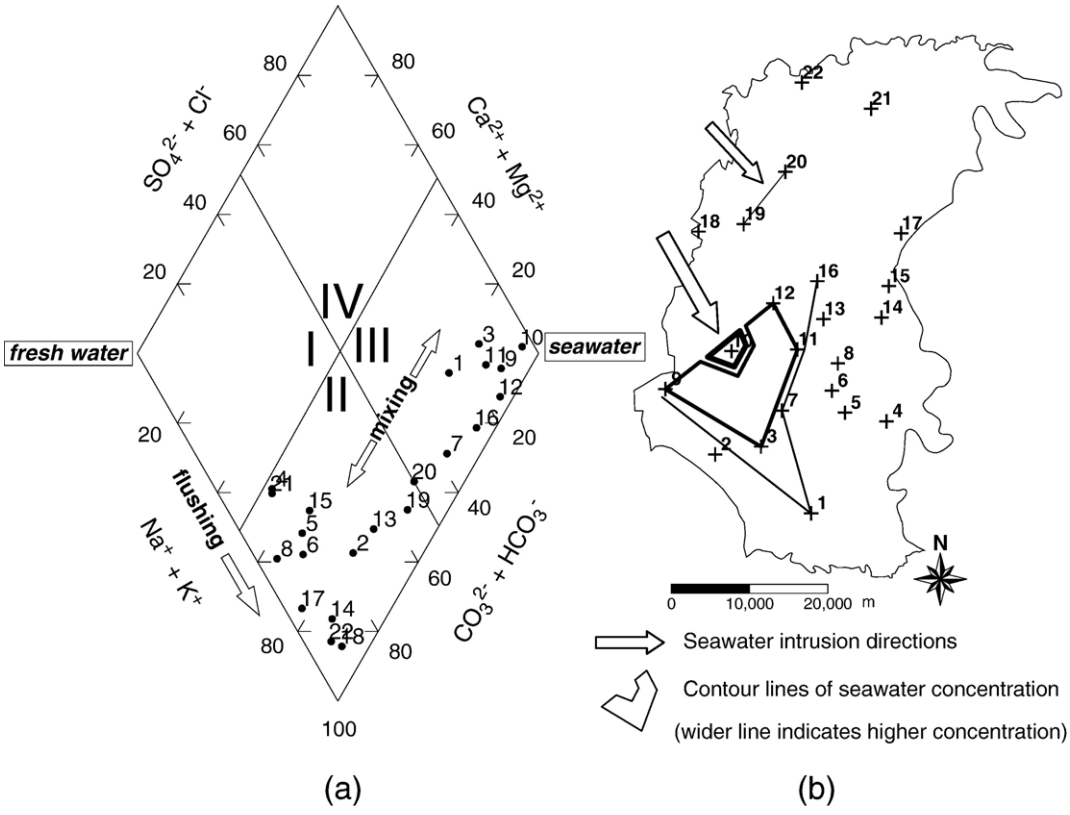

Fig. 3. (a) The Piper plot of the 22 well samples in Aquifer 3 and (b) locations and directions of seawater intrusion.

In MFK, variable X_i is the linear combination of the kth regionalized factor $W^l{}_k(u)$ at the scale of l, and can be expressed as

$$X_i(u) = \sum_l X_i^l(u) = \sum_l \sum_k a_{ik}^l W_k^l(u),$$

where $X_i(u)$ is initially normalized with zero mean and unit variance; $\mathbf{a}^l\mathbf{a}^{lT} = \mathbf{B}^l = \mathbf{Q}^l\mathbf{\Lambda}^l\mathbf{Q}^{lT}$; matrix $\mathbf{Q}^l$ consists of the orthogonal eigenvector of $\mathbf{B}^l$ in column; $\mathbf{\Lambda}^l$ is a diagonal matrix of eigenvalues of $\mathbf{B}^l$, and $\mathbf{a}^l = \mathbf{Q}^l\mathbf{\Lambda}^{l1/2}$. The PCA depicts the values in the first and second columns, the principal component 1 (PC1) and the principal component 2 (PC2), of the calculated $\mathbf{a}^l$ in the correlation circle against the x-axis and the y-axis. And the relationship between the variables is identified by the position in the correlation circle (Wackernagel, 1995).

$X_i(u)$ can be decomposed into sets of spatially uncorrelated factors $W^l{}_k(u)$, and the aim of the mapping step is to yield the regionalized factor $W_k^l(u)_{\}} = \sum_{i=1}^{n} \sum_{n_i=1}^{m} \lambda_{n_ik}^l(u) X_i(u_{n_i})$ by co-kriging. The weight λ_{nik} is then calculated from

$$\begin{cases} \sum_{j=1}^{n} \sum_{n_j=1}^{n} \lambda_{n_ik}^l \gamma_{ij}(u_{n_i} - u_{n_j}) = a_{ik}^l g^l(u_{ni} - u) n_i = 1,\ldots,m \\ \sum_{n_i=1}^{m} \lambda_{n_ik}^l(u) = 0 \qquad ;= l,\ldots,n. \end{cases}$$

Each regionalized factor from kriging was estimated in 37 columns with 57 rows of total 2109 of 1×1 km^2 square cells in the study area.

3. Results and discussion

3.1. Multi-scale analysis

The best fit of experimental variograms and cross-variograms was specified as the sum of three structures, including a nugget-effect term, Gaussian model and spherical model, with ranges of 16 000 m and 32 000 m for the local and regional scales, respectively.

$$\gamma_{ij}(h) = b_{ij}^0 + b_{ij}^1\left(1 - e^{\frac{-3|h|^2}{16000^2}}\right) + b_{ij}^2\left(1.5\frac{|h|}{32000} - 0.5\left(\frac{|h|}{32000}\right)^3\right),$$

where $\gamma_{ij}(h) = b^0{}_{ij} + b^1{}_{ij} + b^2{}_{ij}$ for $h \geq 32{,}000$; $i, j = 1,..,8$; $b^0{}_{ij}$ denotes the nugget effect, $b^1{}_{ij}$ represents the sill of the local-scale Gaussian structure, and $b^2{}_{ij}$ is the sill of the regional-scale spherical structure. Fig. 4 shows that no obvious deviations existed between the experimental variograms and variogram models of eight direct variograms which may be caused by LMC, as mentioned by Goovaerts (1997). This phenomenon indicated that different causes jointly affect the final As enrichment in groundwater with dissimilar ranges of influence. Most direct and cross variogram models have low nugget effects and represent good spatial structure among the variables. These variography results confirm that the conventional correlation coefficient or factor analysis cannot fully identify the spatial correlations among the variables.

Table 3 shows the nugget-effect ratios of all variogram models. The nugget-effect ratio of Alk, Mn and TOC are relatively low. The low nugget-effect ratio indicates the moderate variations within the shortest well distance and low sampling errors. Moreover, the large nugget-effect ratio on the cross variogram with the small nugget-effect ratios on the direct variograms suggests that the nugget effect on the direct variogram results mainly from micro-scale variation. Conversely, the small nugget-effect ratio on the cross variogram associated with large nugget-effect ratios on the direct variograms indicates that measurement errors contribute significantly to the nugget-effect on direct variograms, or that micro-scale variations of both variables are independent (Goovaerts, 1997, p. 103). Table 3 illustrates the cases in which two direct variogram models with small nugget-effect ratios generate a cross variogram model with a large nugget-effect ratio as DO-As, DO-TOC, and ORP-Mn. These cases may imply that small scale reactions operating over distances smaller than the shortest well distance in Aquifer 3 generate the large cross variation. The reductive dissolution of the insoluble manganic oxides in groundwater occurs earlier in the reducing sequence than that of hydrous ferric oxides and sulfate (Smedley and Kinniburgh, 2002). The ORP-sensitive characteristic induces more fractal variation of Mn than can be observed by GMNS. Since Liu et al. (2003) indicated that As is highly correlated with TOC in groundwater, the DO–As and DO–TOC relationships could be described as the variation of DO over distance smaller than the shortest well distance in Aquifer 3 being affected by the organic matter, TOC, in the groundwater. Moreover, the DO variation may influence the enrichment of As in groundwater.

3.2. Principal component analysis

Fig. 5 plots the correlation circles of eight variables. The total variations of groundwater As are 17.3%

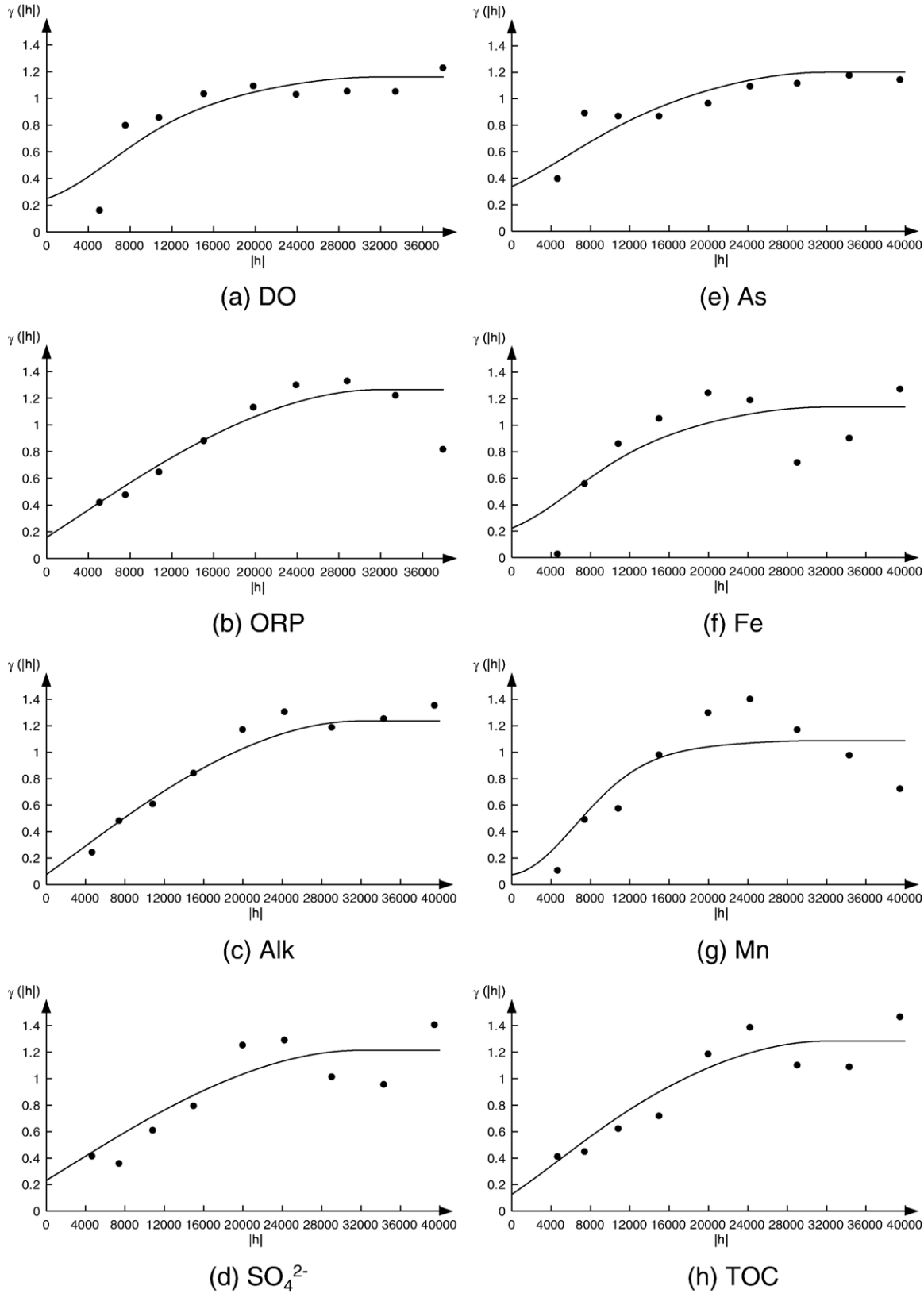

Fig. 4. The experimental variograms and variogram models of (a) DO, (b) ORP, (c) Alk, (d) SO_4^{2-}, (e) As, (f) Fe, (g) Mn, and (h) TOC.

Table 3
Nugget-effect ratio of variogram models

	DO	ORP	Alk	SO_4^{2-}	As	Fe	Mn	TOC
DO	0.215				0.318			0.333
ORP	0.121	0.125					0.262	
Alk	0.043	0.074	0.058					
SO_4^{2-}	0.072	0.067	0.026	0.192				
As	0.318	0.020	0.071	0.276	0.281			
Fe	0.105	0.034	0.127	0.131	0.220	0.196		
Mn	0.149	0.262	0.019	0.045	0.233	0.159	0.070	
TOC	0.333	0.059	0.054	0.120	0.166	0.053	0.023	0.099

generated at the local scale and 64.4% generated at the regional scale, while the nugget effect represents 18.3% variation. The first two principal axes represent 98.30% variation at the regional scale and 93.30% variation at the local scale. The correlation circles at the two scales demonstrated two different types of spatial correlations. These two correlation types implied that the combination of three structures, including the nugget effect, is fundamental to describing the spatial variations of eight variables. The correlation circles can be interpreted by the relative locations where variables are labeled or grouped to estimate the probable relationships between variables. Each axis represents a distinct factor and the variable being positive located indicates the positive influences of the factor on the variable.

At the regional scale (Fig. 5(a)), all variables except DO are closely correlated with PC1. PC1 explains 89.5% of the variation while PC2 explains 8.8% of the variation. The negative correlation of As–DO and As–ORP at the regional scale implies that the reductive condition could enrich As in groundwater. The positive correlation of As–Fe and As–Mn in groundwater can be regarded as an indicator of desorption of the As from reductive dissolution of iron or manganic compounds or reductive liberation from iron–As or manganic–As compounds. Stollenwerk (2003) indicated that adsorption/desorption reactions dominate the As distribution in groundwater. Moreover, in the adsorption/desorption reactions, the isoelectric point (IEP) is referred as an indicator of the capacity of the adsorbing solid. The IEP of a solid mineral represents the pH value in the aqueous solution with zero net particle charge. The most common species of As in a reductive aquifer at neutral pH is H_3AsO_3 (Cherry et al., 1979). The IEP of the adsorption surface is reduced by adsorbing As (Stollenwerk, 2003). If the pH (Alk) exceeds IEP, the net charge of the adsorption surface is negative. Meanwhile the $H_2AsO_3^-$ dominates in groundwater, and thus increasing As is found in groundwater because of the reduced capability of the adsorption surface. The positive correlation between As and Alk therefore can be referred as the desorption reaction of As enrichment in groundwater, from the perspective of acid-base desorption. However, according to Schreiber et al. (2003), the pyrite oxidation leads to positive correlation of As with SO_4^{2-} and Fe in groundwater. In Aquifer 3, pore water contains abundant sulfate over an extended period, and pyrite is easily found in the reductive aquifer (Chen and Liu, 2005). The As is released through desorption of the pyrite oxidation which always dominates in the acid groundwater. Both the redox reaction at the acid condition and the acid-base reaction at the alkaline condition can affect As enrichment, As enrichment appears to mostly be controlled by the later reaction at high pH (Alk).

At the local scale (Fig. 5(b)), PC1 explains 50.4% of the variation while PC2 explains 42.9% of the variation. PC1 illustrates the variation relating to SO_4^{2-} and Mn. For PC2, the explanation of the positive correlation of As–Alk and the negative correlation of As–DO and As–ORP are the same as what is illustrated at the regional scale. The differences between PC1 at the regional scale and PC2 at the local scale are the negative correlation of As–Fe in PC2 at the local scale. Appelo and Postma (1994) proposed that given the constant pH, Alk is negatively correlated with Fe in siderite dissolution. If the negative correlation between Alk and Fe implies the dissolution of the siderite, As can be released from the desorption of siderite which mainly occurs in the acid groundwater. Once the effect of SO_4^{2-} is isolated in the PC1, the dissolution of the siderite can be observed in PC2. Moreover, if DO is limited, the increase of microbial activity (TOC) should induce the positive relationship of TOC–As and the negative correlation of As–DO due to the reduction of DO by TOC (Harvey et al., 2002). The negative correlations of As–DO and As–TOC are interpreted as that the excess DO is introduced outside

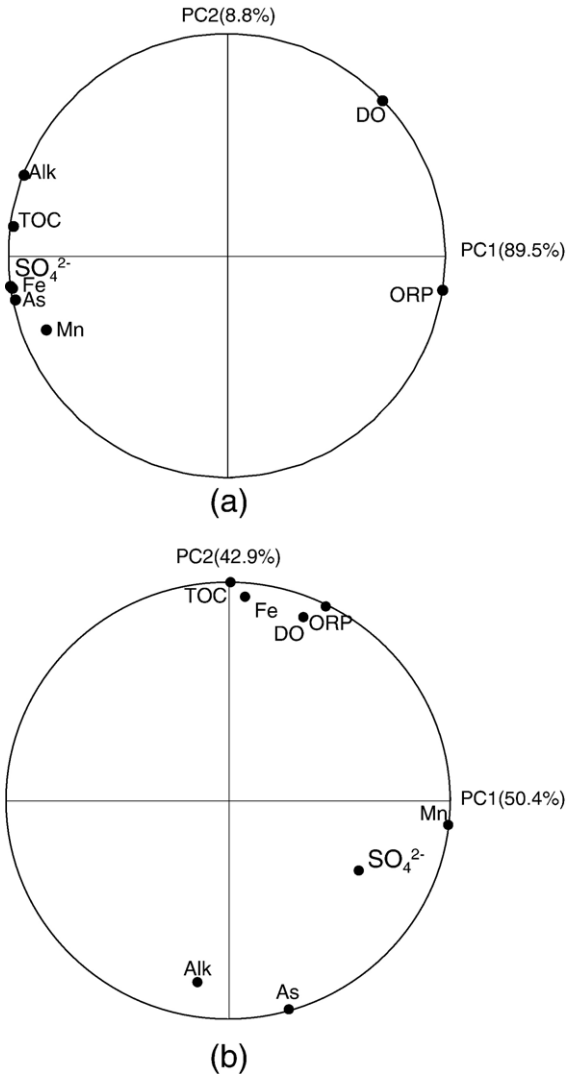

Fig. 5. Correlation circles of variables at (a) the regional scale and (c) the local scale.

the aquifer and the explanation will be confirmed in the mapping results. The organic matters (TOC) can consume the excess DO by oxidizing. The oxidization releases large quantities of carbon dioxide and make the aquifer acid. The acid conditions can increase the release of As from the siderite desorption. Furthermore, the positive correlation between As and Alk as aforementioned can be referred as the desorption of As in the alkaline groundwater in an acid-base reaction. Considering both the siderite dissolution at the acid condition and the acid-base reaction at the alkaline condition can enrich As in groundwater, the release of As in groundwater appears to occur primarily at high pH (Alk). These multivariate analyses show that the multivariate geostatistical method could identify more relationships among groundwater quality variables at different scales than traditional multivariate analysis. The correlations could be used to suggest possible causations. Furthermore, the multivariate geostatistical method generates spatial variation maps that could be combined with additional hydrogeological survey to provide further evidences of causations.

3.3. Mapping regionalized factors

Because As contributed significantly to PC1 at the regional scale and PC2 at the local scale, Fig. 6 maps the regionalized factors of PC1 at the regional scale and PC2 at the local scale to reveal the As variation associated with other variables at different scales. At the regional scale (Fig. 6(a)), a contour line of carbon 14 dating 20 000 years before present shapes a cave-alike area around the high As area. The consistency of locations between the high As area and the cave-like area, obtained from both the hydrogeological survey and the geostatistical interpretation, implies that the groundwater flows too slowly in the cave-alike area to flush the downstream aquifer or to provide extra oxygen. The flushing in the aquifer gradually changes DO in groundwater and creates a more reductive environment in the tail plain compared to the upper plain. The more anoxic the condition of the aquifer, the greater the diffuse release of As to groundwater. At the regional scale, PC1 explains 89.5% of the total spatial variation of As in groundwater, implying that flushing is the main hydrogeological influence on As enrichment in the aquifer.

The local scale is originally selected based on the distance of the seawater intrusion. Smedley and Kinniburgh (2002) mentioned that intrusion of seawater into an aquifer is unlikely to significantly increase As in the intruded area. Fig. 6(b) shows that seawater intrusion weaves through the high-As variation areas in littoral zones since two phenomena cannot occur simultaneously at one location. The movement of As in the aquifers is commonly described as involving the adsorbed As or As compounds being gathered upstream and then transported and released into groundwater via reductive desorption or dissolution downstream. Once freshwater mixes with intruding seawater, the flocculation of Fe oxides at the freshwater-saline convoluted interface appears to reduce As flux into the intruded area. This phenomenon demonstrates that the distribution of As at the local scale is affected by seawater intrusion (Cullen and Reimer, 1989). The conventional factor analysis without considering spatial structures may mislead the spatial correlation between As distribution in groundwater and seawater intrusion in littoral zones as independent factors

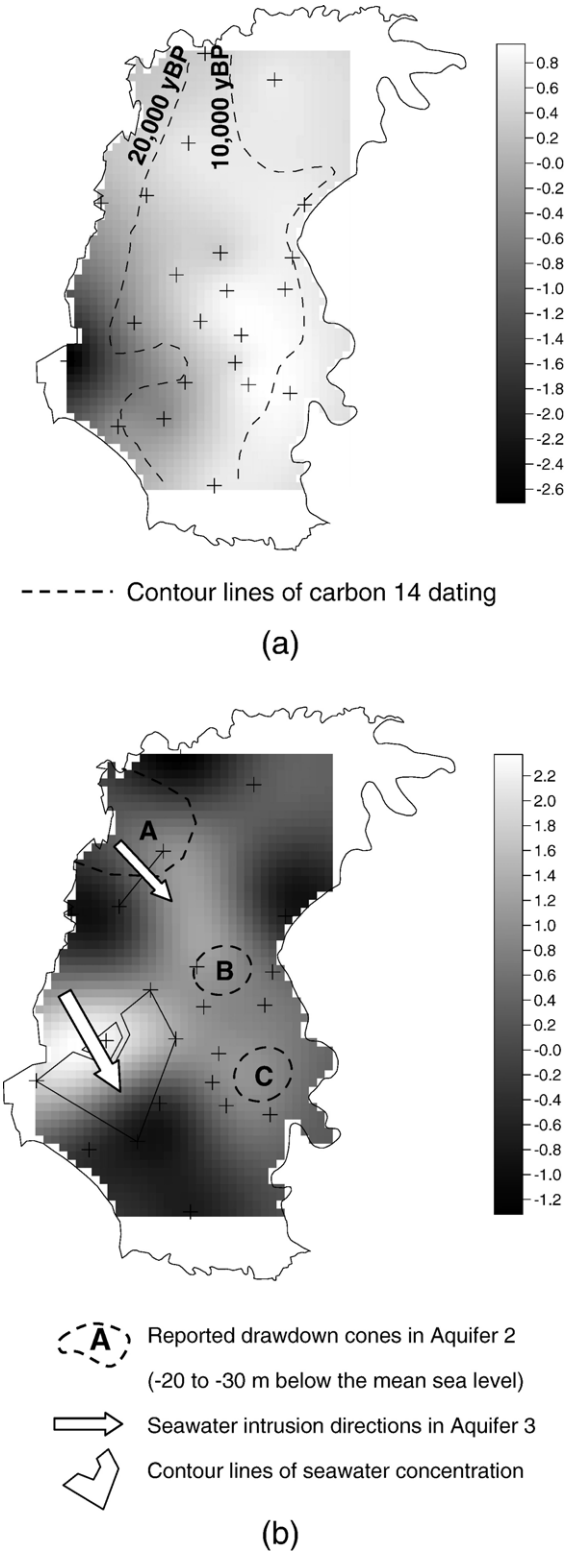

Fig. 6. Regionalized factor maps of (a) PC1 at the regional scale and (b) PC2 at the local scale, where the darkly shaded areas represent high arsenic in groundwater.

(Liu et al., 2003). Fig. 6(b) also shows that three drawdown cones which were measured in Aquifer 2 (Taiwan Sugar Corporation, 2001) all fall within the low As variation areas. Over-extraction of groundwater formed the cones at which high DO is recorded. The excess dissolved oxygen, which may result from the operation of numerous well pumps in the aquifer, may reduce the reductive condition and prevent As being released via reductive dissolution or desorption reactions. Low As around the cones may also be induced by the higher hydraulic gradient around the cones compared to elsewhere. The high hydraulic gradient dilutes the As concentration in groundwater. Mapping regionalized factors provides useful spatial information to help realize the interaction between groundwater quality variations and hydrogeological conditions at different scales.

The analytical results confirm that multivariate factorial kriging which could efficiently extract the spatial variations of variables at different scales and construct spatial correlations between variables, was suitable for analyzing the mechanism of As release in groundwater at different scales. The regions of high As which are affected and restrained by seawater intrusion need further monitoring and limiting of groundwater extraction not only for domestic use but also for aquaculture use, from perspectives of water management and edible safety of aquaculture products.

4. Conclusions

This study applied multivariate factorial kriging to identify the spatial variations of As enrichments with two different scales. While taking the spatial covariance into account, the method differed from the conventional factor analysis and could describe the spatial variations and sources of As variation in groundwater. Additionally, the multi-scale decomposition of As distributions enhanced the correlative delineations between variables at different scales. Moreover, the hydrogeological influences of flushing and seawater intrusion on As enrichment were examined at the regional scale, 32 km, and the local scale, 16 km, respectively, with As and seven variables including DO, ORP, SO_4^{2-}, Alk, Fe, Mn and TOC. The flushing contributed more variation of As enrichment than the seawater intrusion did. The nugget effects suggest that the As variations generated over distance smaller than the shortest well distance are strongly related to DO and TOC. The liberation of As may be partially controlled by the siderite dissolution at the local scale. Moreover, the pyrite oxidation partially affects the As release at the regional scale. The alkalinity overall dominates the As enrichment. Locations with

slow groundwater flow identified by the hydrogeological survey, carbon 14 dating, coincided with the As rich locations. The consistency clarified how the flushing influences As enrichment in groundwater. Furthermore, the seawater intrusion only slightly affected the As enrichment in groundwater owing to that variations at the regional scale dominated the total variations. At the local scale, the distinctly correlative distribution patterns between As and seawater intrusion were identified. The drawdown cones which were induced by the excessive extractions of groundwater fell within the low As area. The excess dissolved oxygen at the same locations might prevent As release from reductive dissolution or desorption reactions. Low As around the cones may also result from that the dissolved As was just diluted by the high hydraulic gradient around the cones.

The analytical results in this study were conducted from the application of MFK in the study area being reductive with clayey deposits of Pleistocene age accompanied with serious seawater intrusion. The interpretive reactions and mechanisms of As enrichment may vary significantly at different places with different hydrogeological conditions. For the risk assessment of cancer mortality using ecological data of categorical As exposures at a particular area (village or town), the MFK which can deconvolute As variations into background terms (flushing affected or hydrogeology correlated) and transient terms (pumping reduced or seawater intrusion affected) can provide more information for predicting the exposure time to a specific As concentration in groundwater.

Acknowledgment

The authors would like to thank Dr. Chen, Wen-Fu in ChiaNan University of Pharmacy and Science for precious suggestions. The authors would also be grateful to thank the National Science Council of Taiwan for financially supporting this research under Contract No. NSC 94-2313-B-041-010.

References

Appelo CA, Postma D. Geochemistry, Groundwater and Pollution. Brookfield AA, Balkema; 1994. 536 pp.

Bourennane H, Salvador-Blanes S, Cornu S, King D. Scale of spatial dependence between chemical properties of topsoil and subsoil over a geologically contrasted area (Massif central, France). Geoderma 2003;112:235–51.

Castrignanò A, Giugliarini L, Risaliti R, Martinelli N. Study of spatial relationships among some soil physica-chemical properties of a field in central Italy using multivariate geostatistics. Geoderma 2000;97:39–60.

Chen SL, Dzeng SR, Yang MH, Chiu KH, Shieh GM, Wai CM. Arsenic species in groundwaters of the blackfoot disease areas, Taiwan. Environ Sci Technol 1994;28:877–81.

Chen WF, Liu TK. Ion activity products of iron sulfides in groundwaters: implications from the Choshui fan-delta, western Taiwan. Geochim Cosmochim Acta 2005;69:3535–44.

Cherry JA, Shaikh AU, Tallman DE, Nicholson RV. Arsenic species as an indicator of redox conditions in groundwater. J Hydrol 1979;43:373–92.

Cressie N. The origins of kriging. Math Geol 1990;22:239–52.

Cullen WR, Reimer KJ. Arsenic speciation in the environment. Chem Rev 1989;89:713–64.

Gaus I, Kinniburgh DG, Talbot JC, Webster R. Geostatistical analysis of arsenic concentration in groundwater in Bangladesh using disjunctive kriging. Environ Geol 2003;44:939–48.

Goovaerts P, Sonnet P, Navarre A. Factorial kriging analysis of springwater contents in the Dyle River Basin, Belgium. Water Resour Res 1993;29:2115–26.

Goovaerts P. Geostatistics for Natural Resources Evaluation. New York: Oxford University Press; 1997. 483 pp.

Goovaerts P, AvRuskin G, Meliker J, Slotnick M, Jacquez G, Nriagu J. Geostatistical modeling of the spatial variability of arsenic in groundwater of southeast Michigan. Water Resour Res 2005a;41: W07013. doi:10.1029/2004WR003705.

Goovaerts P, Jacquez GM, Marcus A. Geostatistical and local cluster analysis of high resolution hyperspectral imagery for detection of anomalies. Remote Sens Environ 2005b;95:351–67.

Goulard M. Inference in coregionalization model. In: Armstrong M, editor. Geostatistics, vol. 1. Dordrecht: Kluwer Academic Publishers; 1989. p. 397–408.

Goulard M, Voltz M. Linear coregionalization model: tools for estimation and choice of cross-variogram matrix. Math Geol 1992;24:269–86.

Guo HR, Valberg PA. Evaluation of the validity of the US EPA's cancer risk assessment of arsenic for low level exposures: a likelihood ratio approach. Environ Geochem Health 1997;19:133–41.

Harvey CF, Swartz CH, Badruzzaman ABM, Koen-Blute N, Yu W, Ali MA, et al. Arsenic mobility and groundwater extraction in Bangladesh. Science 2002;298:1602–6.

Hossain F, Sivakumar B. Spatial pattern of arsenic contamination in shallow wells of Bangladesh: regional geology and nonlinear dynamic. Stoch Environ Res Risk Assess 2006;20:66–76. doi:10.1007/s0047-005-0012-7.

Hsu SK. Plan for a groundwater monitoring network in Taiwan. Hydrogeol J 1998;6:405–15.

Lin YB, Tan YC, Lin YP, Liu CW, Hung CJ. Geostatistical method to delineate anomalies of multi-scale spatial variation in hydrogeological changes due to the ChiChi earthquake in the ChouShui river alluvial fan in Taiwan. Environ Geol 2004;47:102–18.

Lin YP. Multivariate geostatistical methods to identify and map spatial variations of soil heavy metals. Environ Geol 2002;42:1-10.

Liu CW, Lin KH, Kuo YM. Application of factor analysis in the assessment of groundwater quality in a blackfoot disease area in Taiwan. Sci Total Environ 2003;313:77–89.

Liu TK. Radiometric dating and vertical quality variation of groundwater from wells in Taiwan area. Water Resour Agency, Taiwan; 1999. 89 pp. (in Chinese).

National Research Council. Arsenic in Drinking Water: 2001 Update. Washington D.C.: National Academic Press; 2001. 244 pp.

National Research Council. Arsenic in Drinking Water. Washington, D.C.: National Academic Press; 1999. 226 pp.

Pannatier Y. VARIOWIN: Software for Spatial Data Analysis in 2D. New York: Springer-Verlag; 1996. 91 pp.

Reis A, Sousa A, Silva E, Fonseca E. Application of geostatistical methods to arsenic data from soil samples of the Cova dos Mouros mine (Vila Verde–Portugal). Environ Geochem Health 2005;27:259–70.

Reis AP, Sousa AJ, Fonseca EC. Application of geostatistical methods in gold geochemical anomalies identification (Montemor-O-Novo, Portugal). J Geochem Explor 2003;77:45–63.

Schreiber ME, Gotkowitz MB, Simo JA, Freiberg PG. Mechanisms of arsenic release to ground water from naturally occurring sources, eastern Wisconsin. In: Welch A, Stollenwerk K, editors. Arsenic in Groundwater. Boston: Kluwer Academic Publishers; 2003. p. 259–80.

Smedley PL, Kinniburgh DG. A review of the source, behaviour and distribution of arsenic in natural waters. Appl Geochem 2002;17: 517–68.

Stollenwerk KG. Geochemical processes controlling transport of arsenic in groundwater: a review of adsorption. In: Welch A, Stollenwerk K, editors. Arsenic in Groundwater. Boston: Kluwer Academic Publishers; 2003. p. 67-100.

Taiwan Sugar Corporation. Groundwater quality by the Taiwan groundwater monitoring network (3/5). Water Resources Agency, Taiwan; 2001. 203 pp. (in Chinese).

Tseng WP, Chu HM, How SW, Fong JM, Lin CS, Yeh S. Prevalence of skin cancer in an endemic area of chronic arsenicism in Taiwan. J Natl Cancer Inst 1968;40:453–63.

Van Meirvenne M, Goovaerts P. Accounting for spatial dependence in the processing of multitemporal SAR images using factorial kriging. Int J Remote Sens 2002;23:371–87.

Wackernagel H. Multivariate Geostatistics: An Introduction with Applications. Berlin: Springer-Verlag; 1995. 256 pp.

World Health Organization. Guidelines for Drinking-water Quality 2nd ed. Geneva: World Health Organization; 1993.

Yu WH, Harvey CM, Harvey CF. Arsenic in groundwater in Bangladesh: a geosatistical and epidemiological framework for evaluating health effects and potential remedies. Water Resour Res 2003;39:1146. doi:10.1029/2002WR001327.